ACS OMEGA

http://pubs.acs.org/journal/acsodf

Article

Halogenated Coumarin−Chalcones as Multifunctional Monoamine Oxidase-B and Butyrylcholinesterase Inhibitors

Nisha Abdul Rehuman,◆ Jong Min Oh,◆ Lekshmi R. Nath, Ahmed Khames, Mohamed A. Abdelgawad, Nicola Gambacorta, Orazio Nicolotti, Rakesh Kumar Jat, Hoon Kim,* and Bijo Mathew*,◆

Cite This: *ACS Omega* 2021, 6, 28182−28193

Read Online

ACCESS | Metrics & More | Article Recommendations | Supporting Information

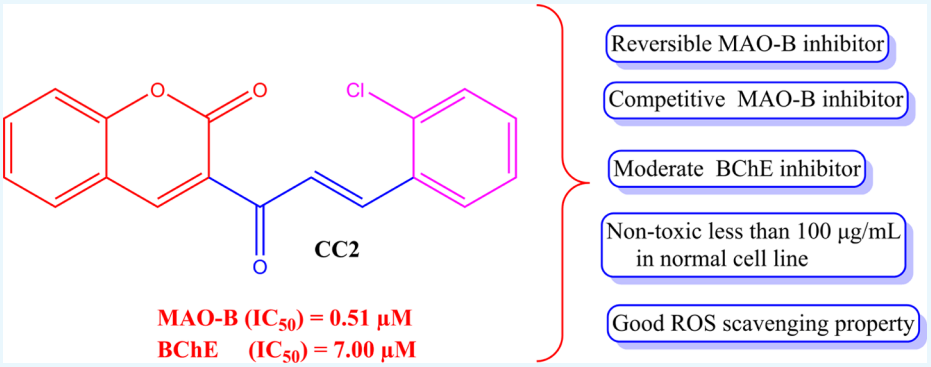

ABSTRACT: A series of halogenated coumarin−chalcones were synthesized, characterized, and their inhibitory activities against monoamine oxidases (MAOs), acetylcholinesterase (AChE), butyrylcholinesterase (BChE), and β-site amyloid precursor protein cleaving enzyme 1 (BACE-1) were evaluated. Compound **CC2** most potently inhibited MAO-B with an IC_{50} value of 0.51 μM, followed by **CC1** (IC_{50} = 0.69 μM), with a selectivity index (SI) of >78.4 and >58.0, respectively, over MAO-A. However, none of the compounds effectively inhibited MAO-A, AChE, and BChE, except for **CC2** and **CC3** inhibiting BChE with IC_{50} values of 7.00 (SI > 5.73 over AChE) and 11.8 μM, respectively. **CC1** and **CC2** were found to be reversible and competitive inhibitors of MAO-B, with K_i values of 0.50 ± 0.06 and 0.53 ± 0.04 μM, respectively, and **CC2** was also a reversible and competitive inhibitor of BChE, with a K_i value of 2.84 ± 0.09 μM. The parallel artificial membrane permeability assay (PAMPA) method showed that lead candidates can cross the blood−brain barrier (BBB). The *in vitro* toxicity analysis on the Vero cell line (Normal African green monkey kidney epithelial cells) by MTT confirmed that both **CC1** and **CC2** were nontoxic up to 100 μg/mL, which is almost equivalent to 100 times of their effective concentration used in biological studies. In addition, **CC1** and **CC2** attenuated H_2O_2-induced cellular damage via their reactive oxygen species (ROS) scavenging effect. These results suggest that **CC1** and **CC2** are selective and competitive inhibitors of MAO-B, and that **CC2** is a selective and competitive inhibitor of BChE. Molecular docking studies of lead compounds provided the possible type of interactions in the targeted enzymes. Based on the findings, both compounds, **CC1** and **CC2**, can be considered plausible drug candidates against neurodegenerative disorders.

1. INTRODUCTION

Alzheimer's disease (AD) is a neurodegenerative disorder that is genetically complex, irreversible, and slowly progressive in the older population.[1] Due to the multifactorial pathogenesis of AD, researchers have focused on the development of multitarget-directed ligands (MTDL).[2] Studies have been proposed for a novel paradigm shift to develop a therapeutic molecule that acts on different targets of the disease with different persuasion levels.[3,4] Understanding the etiology and design of scaffolds by molecular hybridization induces potent MTDL development. The putative factors included in the pathology of AD are oxidative/nitrosative stress, altered apoptosis, mitochondrial damage, neuroinflammation of the immune system, genetics, Ca^{2+} and metal dyshomeostasis, autophagy, and enzymes such as cholinesterases (ChEs), β-site amyloid precursor protein cleaving enzyme 1 (β-secretase, BACE-1), and monoamine oxidases (MAOs).

MAOs have two types of enzymes (MAO-A and MAO-B), which are responsible for the degradation of neurotransmitters like epinephrine, norepinephrine, dopamine, and serotonin present in peripheral and central tissues.[3,4] One of the major

Received: August 8, 2021
Accepted: September 24, 2021
Published: October 12, 2021

Table 1. Inhibitions of Recombinant Human MAO-A, MAO-B, AChE, BChE, and BACE-1 by Compounds of the CC Series

	residual activity at 10 μM (%)					IC_{50} (μM)[a]				
compounds	MAO-A	MAO-B	AChE[c]	BChE	BACE-1	MAO-A	MAO-B	AChE	BChE	SI[b]
CC1	94.8 ± 1.8	10.4 ± 4.4	86.0 ± 3.6	66.1 ± 1.5	74.6 ± 0.2	>40	0.69 ± 0.09	>40	>40	>58.0
CC2	76.6 ± 1.8	19.8 ± 5.9	69.4 ± 3.6	43.9 ± 3.7	61.1 ± 1.0	>40	0.51 ± 0.29	40.1 ± 0.12	7.00 ± 0.02	>78.4
CC3	95.5 ± 0.9	34.9 ± 0.7	77.1 ± 1.8	55.8 ± 4.1	91.0 ± 0.8	>40	1.53 ± 0.39	>40	11.80 ± 0.54	>26.1
CC4	86.8 ± 0.8	60.1 ± 4.5	76.9 ± 9.9	69.9 ± 3.9	78.1 ± 0.6	>40	26.20 ± 0.22	>40	>40	>1.53
CC5	86.8 ± 5.7	69.6 ± 5.4	78.2 ± 0.0	62.1 ± 2.2	92.5 ± 0.8	>40	23.60 ± 1.55	>40	>40	>1.69
CC6	86.2 ± 0.0	95.6 ± 4.5	73.7 ± 6.4	63.2 ± 6.4	92.8 ± 0.8	>40	33.60 ± 1.21	>40	>40	>1.19
CC7	87.3 ± 7.7	31.6 ± 1.7	69.6 ± 0.5	85.4 ± 6.0	75.6 ± 0.2	>40	2.50 ± 0.30	>40	>40	>16.0
CC8	83.1 ± 3.4	37.7 ± 1.2	69.6 ± 0.5	75.0 ± 3.0	89.1 ± 0.3	>40	7.76 ± 0.81	>40	>40	>5.15
CC9	98.8 ± 3.4	39.3 ± 4.6	75.5 ± 0.5	55.7 ± 3.4	80.8 ± 0.4	>40	3.61 ± 0.12	>40	30.0 ± 2.00	>11.1
CC10	88.1 ± 5.1	30.8 ± 1.2	76.7 ± 3.8	75.0 ± 6.3	81.2 ± 0.2	>40	3.36 ± 0.71	>40	>40	>11.9
toloxatone						1.08 ± 0.03				
lazabemide							0.11 ± 0.02			
clorgyline						0.0070 ± 0.0007				
pargyline							0.14 ± 0.01			
tacrine								0.27 ± 0.02	0.060 ± 0.002	
donepezil								0.0095 ± 0.0019	0.180 ± 0.004	

[a]Results are expressed as means ± standard errors of duplicate or triplicate experiments. [b]Selectivity index (SI) values are expressed for MAO-B as compared with MAO-A. [c]Values for reference compounds were determined after preincubation for 30 min with enzymes.

https://doi.org/10.1021/acsomega.1c04252
ACS Omega 2021, 6, 28182−28193

etiologies of neurodegenerative disease is oxidative damage of the brain, which is likely to be caused by the degradation of neurotransmitters. Reactive oxygen species (ROS) and hydrogen peroxide are produced by the degradation of amines, which are responsible for oxidative damage. Other than MAOs, ChEs, such as acetylcholinesterase (AChE) and butyrylcholinesterase (BChE), also play important roles in the etiology of AD.[5−9] Research studies have claimed that multitargeting drugs provide better efficacy than single-targeting drugs due to the multifactorial pathogenesis of AD.[10−13]

Drugs like donepezil (AChE inhibitor) increase the cholinergic system by inhibiting the enzyme acetylcholinesterase.[14] On the other side, the *N*-methyl-D-aspartate (NMDA) receptor antagonist (memantine) acts by attenuating glutamate receptor activity.[15] For AD therapy, the aforementioned drugs are insufficient. Therefore, the aim of the study is to develop a new class of drugs to reduce this impairment of their causative reason. Currently, the available drugs are single targets that help to improve cognition and memory loss. However, the single-target drugs are poor curative agents for AD. Due to the complex pathogenesis of AD, a multitarget drug could be more effective (synergistic effect) in leading to an improvement of cognition and memory.[16,17] It has been suggested that chalcones are better pharmacophores for the development of multitarget ligands for targeting neurodegenerative disorders.[18−20]

Coumarin is a bicyclic heterocyclic compound comprising an aromatic ring fused to a 6-member lactone ring, which is chemically 1-benzopyran-2-one.[21] Both the synthetic and natural coumarin compounds showed versatile pharmacological activities, such as antioxidant,[12−24] antimicrobial,[25] anticarcinogenic,[26,27] MAO-B inhibiting,[28] and anti-ChE activities.[29,30] Chalcones are chemically olefinic (containing α,β-unsaturated ketones) compounds formed with a linkage between the two aryl/hetero aryl moieties. The presence of electron-withdrawing and electron-donating groups on ring **A** and ring **B** greatly influences MAO-B and AChE inhibitory activities, and the orientation of the electron-withdrawing and electron-donating groups greatly influences the electrophilic character of the Michael acceptor.[31−48] Recent studies have reported that the presence of a halogen atom on ring B results in a compound with a highly selective MAO-B inhibitor.[49,50]

Due to the presence of olefinic linkage, chalcones exist both as *cis* and *trans*, where *trans* is more stable than *cis*.[51] The presence of electron-withdrawing or electron-donating functional groups present in the benzene ring shows the fluorescent property of chalcones.[52] Michael acceptors are electrophiles that are biologically and actively involved in the signaling pathway in cells. The α,β-unsaturated ketone present in the chalcone was perceived as a Michael acceptor. The electrophile present in the chalcone forms a covalent bond with the thiol or sulfhydryl group present in cysteine form, Michael adduct.[53] Recently, Moya-Alvarado et al. synthesized and evaluated the MAO-B inhibitory profiles of some methoxy-bearing coumarin-based chalcones.[54] Therefore, in this study, we synthesized a group of coumarin−chalcones and studied their ability to inhibit MAOs, ChEs, and BACE-1, which are responsible for neurodegenerative diseases. The most promising lead molecules were further evaluated for their biological safety profiles and ROS assay using the Vero cells *in vitro* system.

2. RESULTS AND DISCUSSION

2.1. Synthesis. The synthesis of halogenated coumarin−chalcones was done by the condensation of 3-acetylcoumarin with various substituted halogenated benzaldehydes by Claisen−Schmidt condensation.[55,56] ^{1}H NMR of **CC2** showed the sharp doublet peak for Hα and Hβ at 8.29−8.26 and 7.95−7.92, respectively. A large coupling constant of 15−16 Hz of the double bond of chalcones confirmed its *trans* conformation.[57] The presence of a sharp deshielded sp^2 carbonyl carbon at 186.24 δ in the ^{13}C-NMR of **CC2** gave the confirmation of the α,β-unsaturated ketone system. The HRMS analysis showed the molecular weights of the targeted compounds (Supporting Information Figures S1−S21).

2.2. Inhibitory Activities Against MAOs, AChE, BChE, and BACE-1. Among the 10 derivatives tested, seven compounds showed residual activities of <50% for MAO-B at 10 μM. However, all compounds weakly inhibited MAO-A, AChE, BChE, and BACE-1, except that **CC2** inhibited BChE with a residual activity of <50% at 10 μM (Table 1). Compound **CC2** most potently inhibited MAO-B with an IC$_{50}$ value of 0.51 μM, followed by **CC1** (IC$_{50}$ = 0.69 μM), with selectivity index (SI) values of >78.4 and >58.0, respectively, over MAO-A. Moreover, **CC2** potently inhibited BChE (IC$_{50}$ = 7.00 μM). All compounds weakly inhibited MAO-A, AChE, and BACE-1 with >50% of residual activity at 10 μM (Table 1). From the analysis of the synthesized compounds, the structure−activity relationship (SAR) indicates that the orientation of the halogen atoms at the various positions of phenyl ring B greatly influences MAO-B inhibition. Considering the halogen substitution on the phenyl B ring, chlorine at the *ortho* position leads to greater MAO-B inhibition compared to bromine and fluorine substitution.

The rotatable bond in the α,β-unsaturated ketone was perceived as a Michael acceptor, which is responsible for binding with different enzyme targets.[18] This depends on the bulkiness and nature of the groups attached on rings **A** and **B** of the chalcones, which greatly influence the binding interaction in the inhibitor cavity of the enzymes. It has been reported that in chalcones, the presence of electron-withdrawing groups (F, Cl, Br) and electron-donating groups (methyl, ethyl, methoxy, dimethylamino) at the *para* position of phenyl ring **B** lead to better MAO-B inhibition compared to MAO-A.[19] For better AChE inhibition, a nitrogen-derived pharmacophore or methyl-containing group is essential in chalcones.[18]

This study shows that (i) the unsubstituted phenyl **B** ring shows better MAO-B inhibition with an IC$_{50}$ value of 0.69 μM, having high residual activities for MAO-A, AChE, BChE, and BACE-1 (94.8, 86.8, 66.1, and 74.6%, respectively); (ii) the polarizability of the halogen atoms at the *ortho* position of the phenyl ring **B** shows MAO-B inhibition with IC$_{50}$ values of 0.51, 7.76, and 23.6 μM for 2-Cl, 2-F, and 2-Br, respectively, i.e., Cl > F > Br in order, and with BACE-1 residual activities of 61.1, 89.1, and 92.5%, respectively, at 10 μM; (iii) moving the halogen atom Cl from *ortho* to *meta* position leads to less MAO-B inhibition (IC$_{50}$ of 3-Cl = 1.50 μM); (iv) lipophilic atoms Br and F at the *para* position of the phenyl ring **B** show better MAO-B inhibition compared to the atoms at the *meta* position with IC$_{50}$ values of 3.36 and 2.50 μM for 4-F and 4-Br, respectively; (v) the presence of the electron-withdrawing Cl atom at the *ortho* and *meta* positions leads to BChE inhibition with IC$_{50}$ values of 7.00 and 11.8 μM for 2-Cl and 3-Cl,

https://doi.org/10.1021/acsomega.1c04252
ACS Omega 2021, 6, 28182−28193

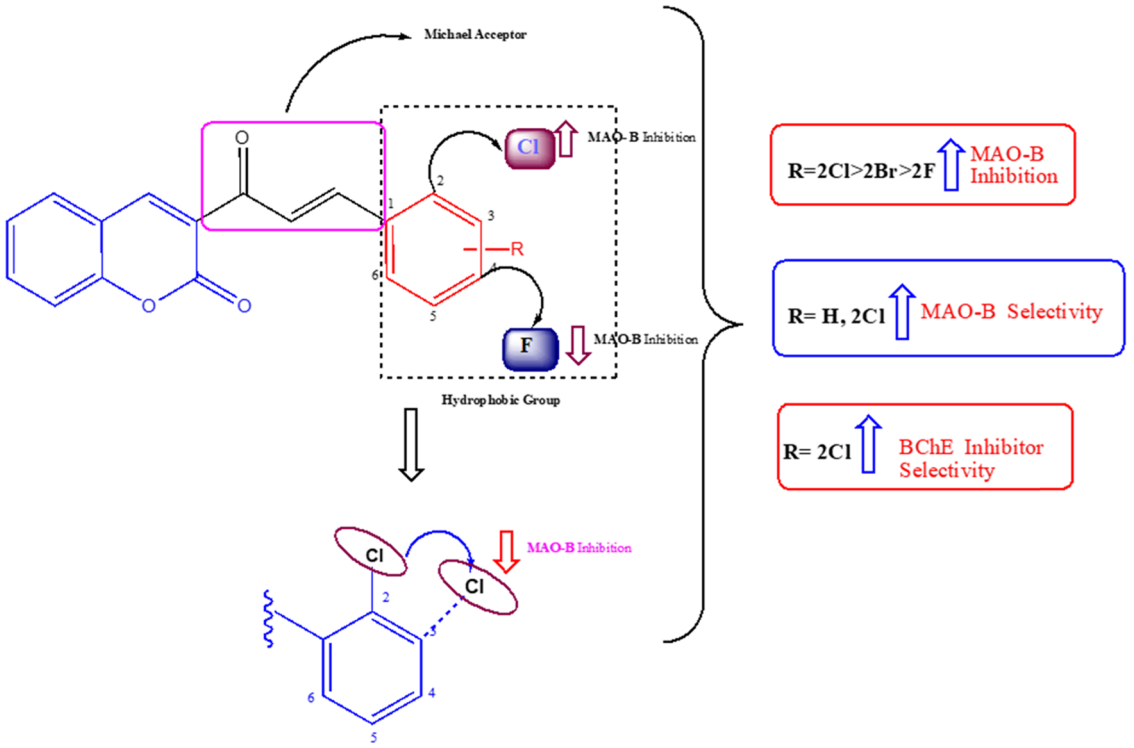

Figure 1. SAR analyses of halogenated coumarin−chalcones.

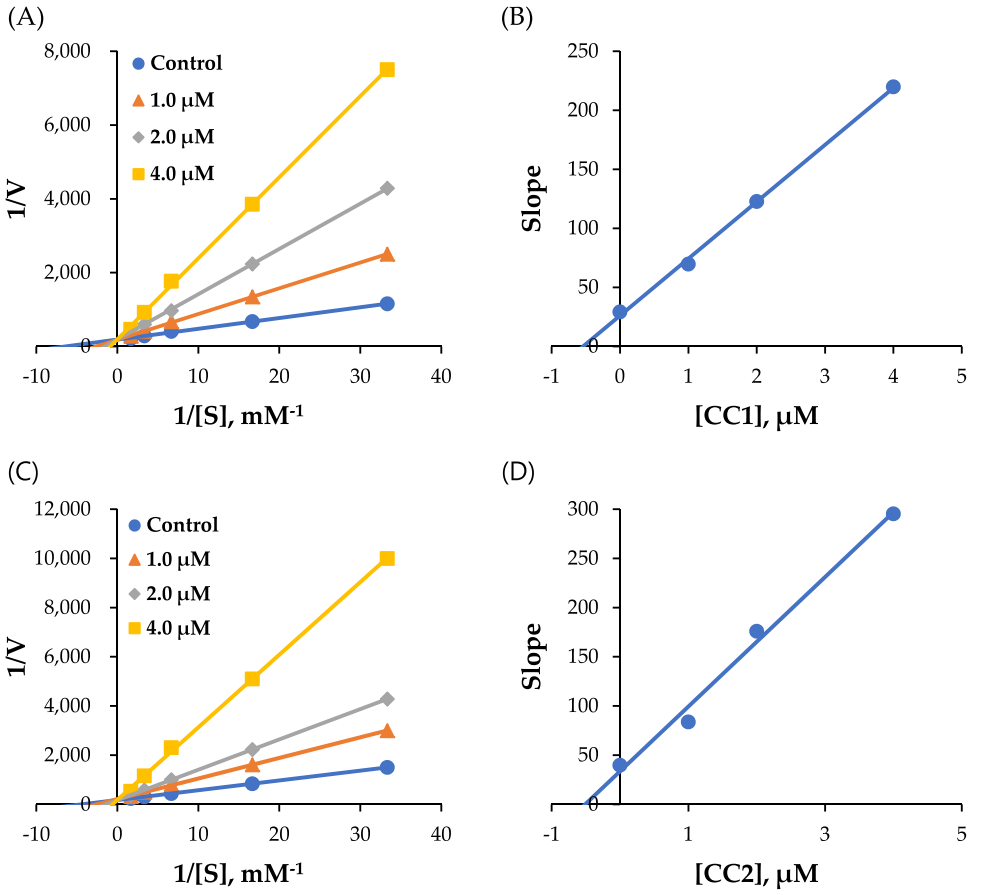

Figure 2. Lineweaver−Burk plots for MAO-B inhibition by **CC1** and **CC2** (A, C) and their respective secondary plots (B, D) of the slopes vs inhibitor concentrations.

https://doi.org/10.1021/acsomega.1c04252
ACS Omega 2021, 6, 28182−28193

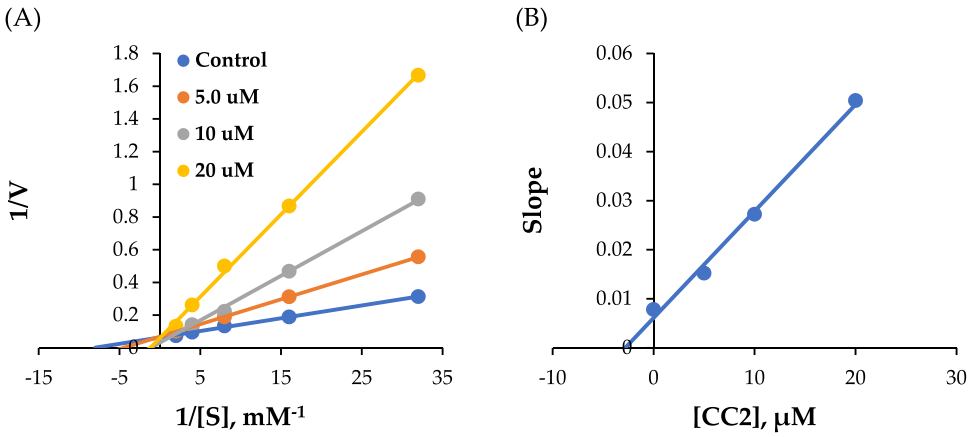

Figure 3. Lineweaver–Burk plots for BChE inhibition by **CC2** (A) and their respective secondary plots (B) of the slopes vs inhibitor concentrations.

respectively. The fluorine atom at the *meta* position leads to BChE inhibition with an IC_{50} value of 30.0 μM. The SAR study concluded that all of the halogen-substituted compounds moderately inhibited MAO-B compared to MAO-A inhibition. Regarding AChE inhibition, the Cl atom at the *ortho* position of phenyl ring **B** shows an IC_{50} value of 40 μM.

For the development of dual-acting MAO-B and AChE inhibitors, researchers have used MTDL strategies. In AD, the production of neurotoxic free radicals, the production of β-amyloid, and the degradation of acetylcholine are caused by the enzymes MAO-B, AChE, and BACE-1, respectively; thus, studies have focused on the development of highly selective ligands to the target enzymes. BACE-1 inhibition from the coumarin–chalcones is not much promising. The lead molecule **CC2** showed a moderate residual activity of 61.1% for BACE-1 at 10 μM. This study focused on the development of coumarin-based halogen-substituted chalcones on MAO-A, MAO-B, AChE, BChE, and BACE-1. Our results concluded that the lead molecules **CC1** and **CC2** selectively inhibit MAO-B at the submicromolar level, and **CC2** moderately inhibits both AChE and BChE. The SAR is depicted in Figure 1.

2.3. Kinetics of MAO-B and BChE Inhibitions. In kinetic studies of MAO-B by **CC1** and **CC2**, Lineweaver–Burk and secondary plots showed that **CC1** and **CC2** were competitive inhibitors for MAO-B (Figure 2A,C), with K_i values of 0.50 ± 0.06 and 0.53 ± 0.04 μM, respectively (Figure 2B,D). In kinetic studies of BChE by **CC2**, Lineweaver–Burk and secondary plots showed that **CC2** was a competitive inhibitor of BChE (Figure 3A), with K_i values of 2.84 ± 0.09 μM (Figure 3B).

2.4. Reversibility Studies. In reversibility experiments using dialysis methods, the inhibition of MAO-B by **CC1** was recovered from 37.6 (value of AU) to 87.9% (value of AD), and **CC2** was also recovered from 37.7 (AU) to 90.2% (AD) (Figure 4). The recovery values were similar to those of the reversible reference lazabemide (from 36.8 to 85.5%). Inhibition of MAO-B by the irreversible inhibitor pargyline was not recovered (from 34.2 to 26.9%). In addition, inhibition of BChE by **CC2** was recovered from 26.6 (value of AU) to 72.1% (value of AD) (Figure 5). The recovery value was similar to that of the reversible reference donepezil (from 26.8 to 85.4%). These experiments showed that inhibitions of MAO-B by **CC1** and **CC2** were recovered to the reversible reference level, and **CC2** was also recovered to the reversible

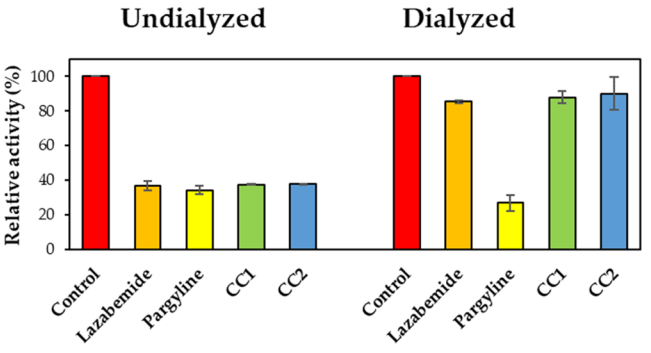

Figure 4. Recoveries of MAO-B inhibitions by **CC1** and **CC2** using dialysis experiments.

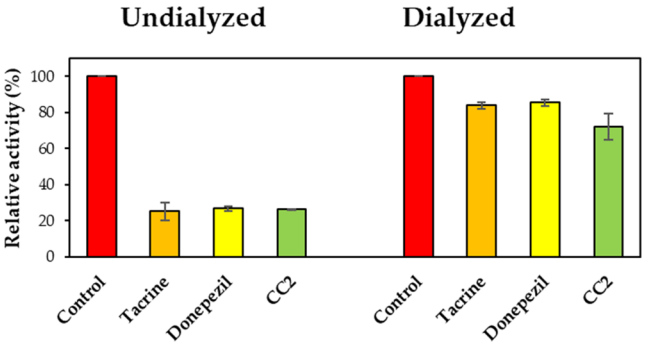

Figure 5. Recoveries of BChE inhibitions by **CC2** using dialysis experiments.

reference level by BChE, indicating that **CC1** and **CC2** are reversible inhibitors of MAO-B, and **CC2** is a reversible inhibitor of BChE.

Reversible inhibitors of monoamine oxidase selectively and reversibly inhibit MAO enzymes. Compared to irreversible MAO inhibitors, reversible ones are safe in single-drug overdoses due to their reversibility.[58] Irreversible MAO inhibitors cause long-term enzyme inactivation, thus causing serious side effects that induce serotonin syndrome. For reversible MAO inhibitors, the formation of high levels of endogenous ligands can be decreased by displacing MAO inhibitors from the active site. Therefore, the discovery of selective and reversible MAO inhibitors is beneficial for the treatment of CNS disorders, particularly AD.[59] Current studies

https://doi.org/10.1021/acsomega.1c04252
ACS Omega 2021, 6, 28182–28193

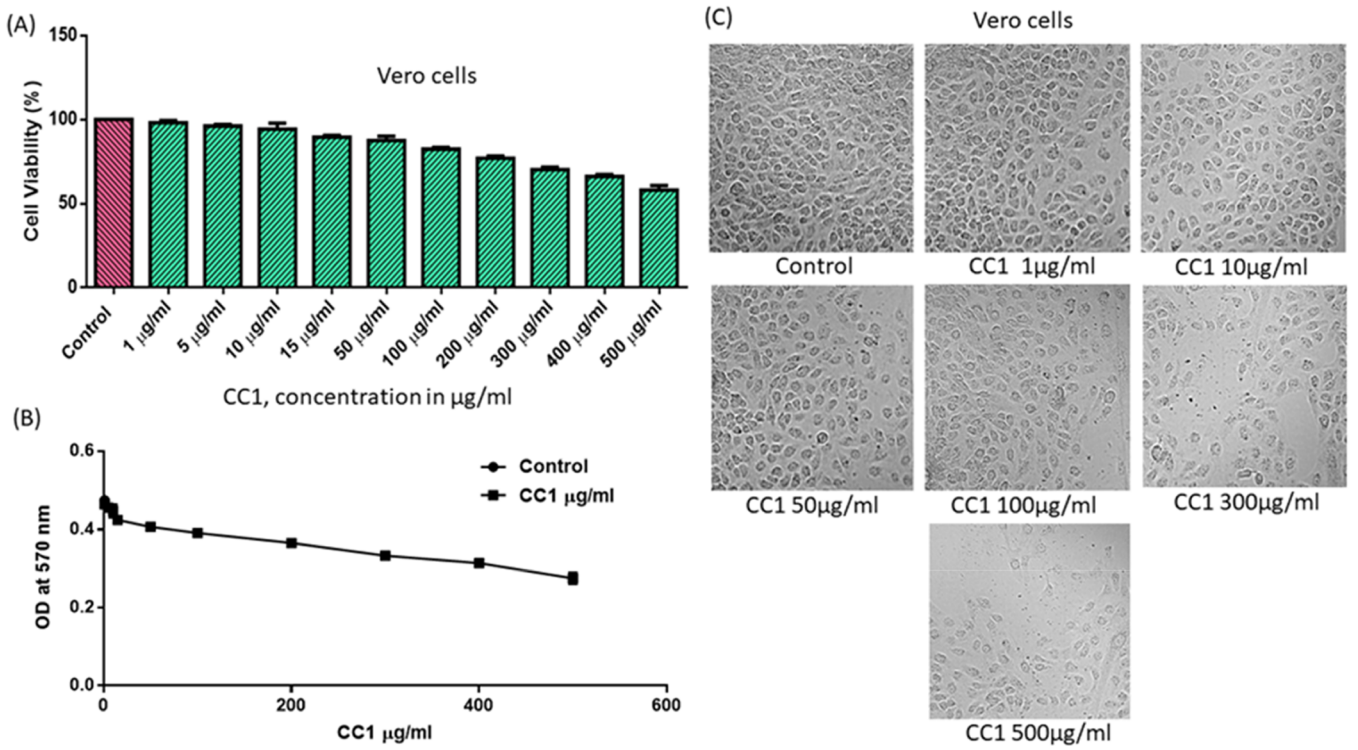

Figure 6. Effect of **CC1** on Vero cell viability. (A) Cell viability; a high viability (>80%) up to 100 μg/mL (363.4 μM). (B) Representation of a dose−response curve with IC_{50} 119.3 μg/mL (431.9 μM). (C) Morphological observation of Vero cells with different concentrations under a phase-contrast microscope, exposed for 48 h. The control value was taken as 100%, and the data were presented as means ± SE from three independent experiments.

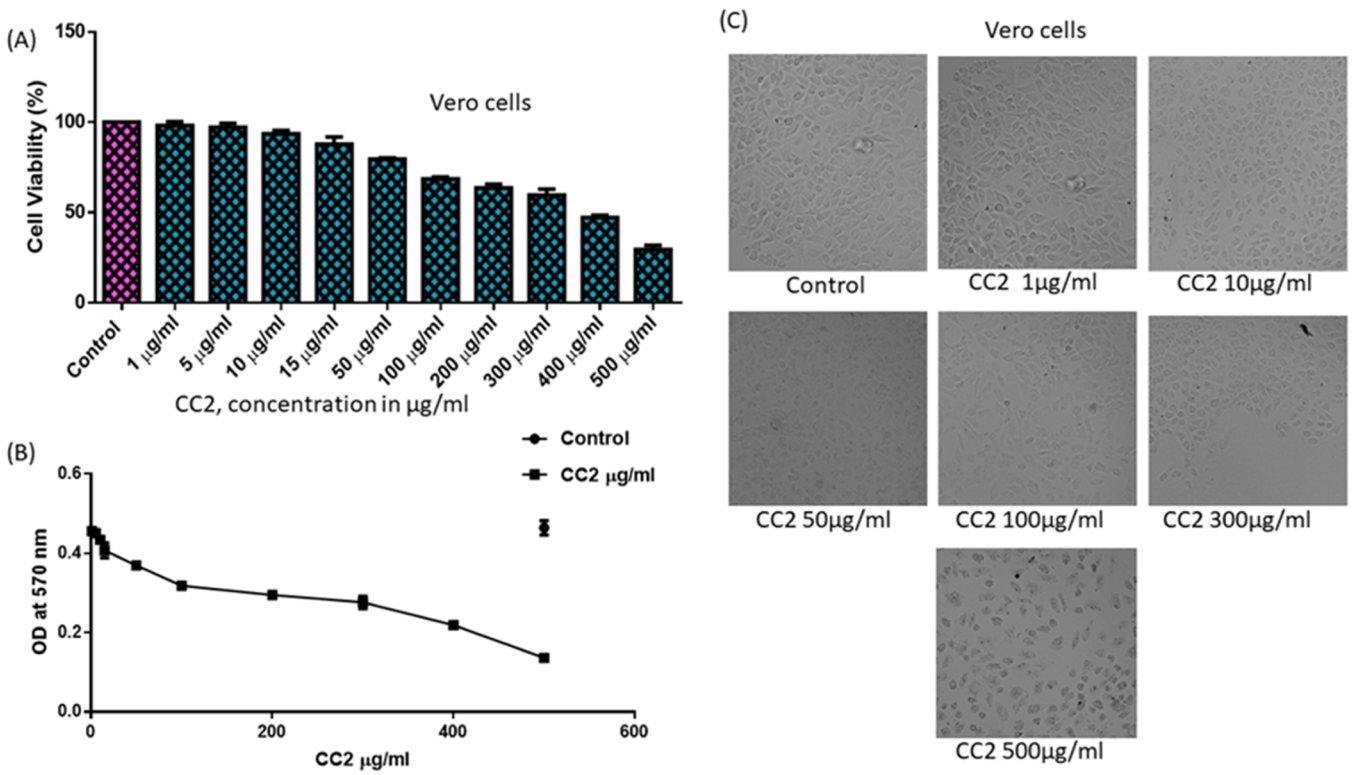

Figure 7. Effect of **CC2** on Vero cell viability. (A) Cell viability; a high viability (>70%) up to 100 μg/mL (321.9 μM). (B) Representation of a dose−response curve with IC_{50} 141.7 μg/mL (456.1 μM). (C) Morphological observation of Vero cells with different concentrations under a phase-contrast microscope, exposed for 48 h. The control value was taken as 100%, and the data were presented as means ± SE from three independent experiments.

https://doi.org/10.1021/acsomega.1c04252
ACS Omega 2021, 6, 28182−28193

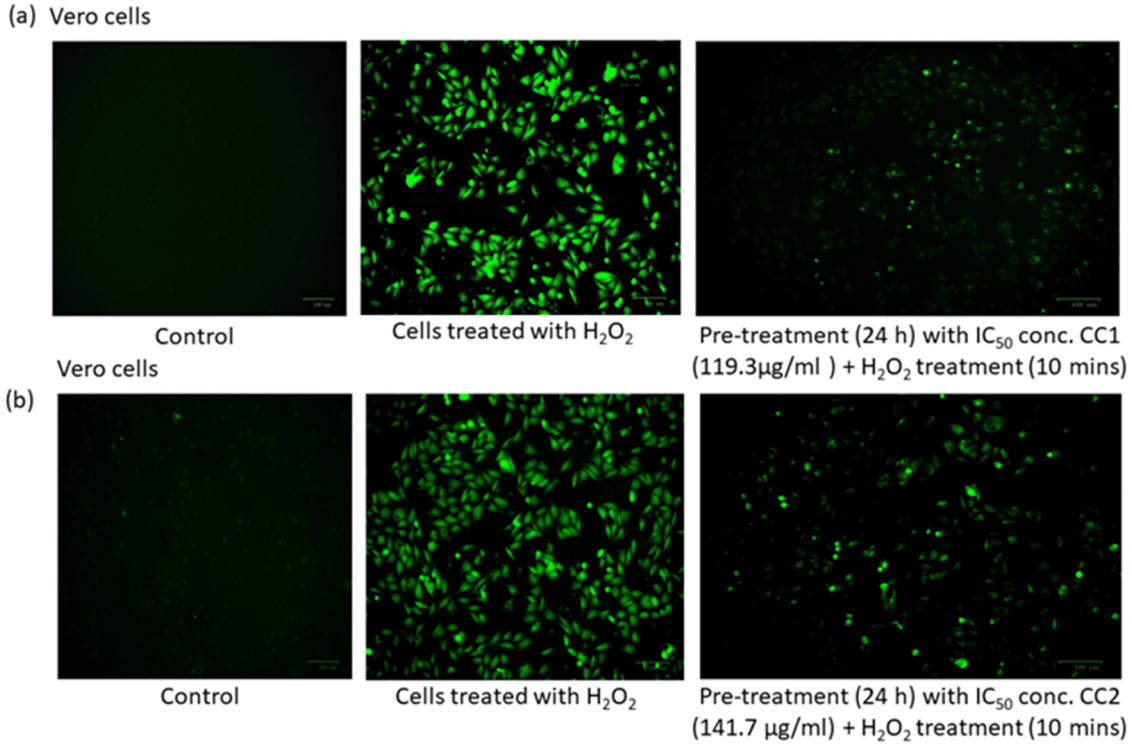

Figure 8. Effects of **CC1** (a) and **CC2** (b) on Vero cells treated with H_2O_2 to generate ROS. Vero cells were treated with 100 μg/mL of 30% H_2O_2 for 10 min, and the production of ROS was evaluated immediately.

on the reversible inhibition of MAO-B by **CC1** and **CC2** propose minimal disruption to the target.

2.5. *In Vitro* Toxicity Evaluation. We further tested the *in vitro* toxicity of the compounds **CC1** and **CC2** on a normal epithelial cell line from the kidney of an African green monkey (Vero Cells) by MTT to prove the biological safety. The Vero cells were exposed to different concentrations (1−500 μg/mL) of the tested compounds for 48 h, and the relative cell viability was calculated as absorbance measured at λ_{max} 540 nm using an ELISA microplate reader. The results indicated that the compounds induced concentration-dependent cell toxicity at the indicated time point of 48 h. It was found that more than 80% of the cells were even viable up to 100 μg/mL (363.4 μM) for **CC1** (Figure 6A), whereas **CC2** showed an approximate cell viability of 70% at the same concentration level (321.9 μM) (Figure 7A). The IC_{50} values of **CC1** and **CC2** were calculated from a dose−response curve plotted using GraphPad Prism 6.0 software. The IC_{50} values were 119.3 μg/mL (431.9 μM) for **CC1** (Figure 6B) and 141.7 μg/mL (456.1 μM) for **CC2** (Figure 7B), whereas the EC_{50} values of the respective compounds were below 1 μM. We also examined whether the addition of **CC1** and **CC2** to Vero cells had any effect on the cellular morphology using phase-contrast microscopy. The membrane integrity and reduction in cell numbers associated with cellular viability are also demonstrated morphologically on Vero cells. When **CC1**- and **CC2**-treated cells were compared with their respective controls, no distinct signs of toxicity were observed at 100 μg/mL (Figures 6C and 7C). The cells exposed to higher concentrations (300 and 500 μg/mL) showed marked morphological alterations typically associated with cytotoxicity, such as marked reduction in cellular density, cellular shrinkage, and blebbing. This study showed that **CC1** and **CC2** were not toxic for Vero cells up to a concentration of 100 μg/mL, which is almost equivalent to 100 times of their effective concentration in the biological study.

2.6. ROS Assay. To further explore the intracellular ROS scavenging effect of **CC1** and **CC2**, Vero cells were exposed to H_2O_2 for excess ROS generation for 10 min, and the images were taken under a fluorescence microscope.[60] The IC_{50} concentrations of **CC1** and **CC2** (119.3 and 141.7 μg/mL, respectively) showed excellent ROS scavenging activity compared to that of the H_2O_2-treated control cells alone. These results indicate that **CC1** and **CC2** treatment inhibited intracellular ROS generation in H_2O_2-treated Vero cells. A decrease in ROS level was evaluated as a decrease in the intensity of fluorescence after 24 h of drug treatment, indicating the balance of prooxidant and antioxidant levels in the cell system (Figure 8A,B). Many studies have indicated that a high concentration of ROS leads to neural damage via oxidative stress in the brain during neurodegenerative disease.[61] Both compounds can effectively regulate the ROS production induced by H_2O_2 treatment with its significant radical scavenging activity.

2.7. Computational Studies. To investigate the effect of interactions between compounds **CC1** and **CC2** toward MAOs, in silico analyses were performed, and the docking score and MM-GBSA values obtained from computational studies are provided in Table 2. For completeness, the reference values concerning cognate ligands within the targets are provided in Tables S1 and S2 of the Supporting Information.

The main interactions engaged from compounds **CC1** and **CC2** toward MAO-A are shown in Figure 9. Interestingly, the coumarin ring can interact with Y407 through $\pi-\pi$ contacts being placed within the hydrophobic region made up of FAD, Y407, and Y444, while the styrene moiety establishes $\pi-\pi$ interaction with F208.

https://doi.org/10.1021/acsomega.1c04252
ACS Omega 2021, 6, 28182−28193

Table 2. Docking Score and MM-GBSA Values of Compounds CC1 and CC2 toward MAOs

	MAO-A		MAO-B	
compound	docking score (kcal/mol)	MM-GBSA (kcal/mol)	docking score (kcal/mol)	MM-GBSA (kcal/mol)
CC1	−8.70	−32.11	−10.47	−49.54
CC2	−8.55	−24.60	−10.47	−50.52

Given the binding modes toward MAO-B, the coumarin ring can make $\pi-\pi$ interactions with Y398 that is trapped in the aromatic cage formed by FAD, Y398, and Y435 (Figure 10). Furthermore, the carbonyl group of the chalcone bridge can form a hydrogen bond with the hydroxyl group of the side chain of the Y326 MAO-B selective residue.

The molecular docking and MM-GBSA analyses were helpful in explaining the binding toward MAO-A and MAO-B at a molecular level following the experimental IC_{50} inhibition data. The interaction of **CC1** and **CC2** with the selective MAO-B residue Y326 is crucial for binding toward MAO-B. Furthermore, both the docking score and MM-GBSA values confirmed the observed binding mode and the interactions toward MAO-B. In particular, with the MM-GBSA method, it was possible to select docking poses and perform a more accurate rescoring, considering some empirical corrections concerning both polar and hydrophobic interactions, thus providing more reliable results. For the sake of completeness, computational simulations have been performed also towards AChE and BChE targets: docking score and MM-GBSA values can be retrieved in Table S2 of the Supporting Information. Interestingly, compounds **CC1** and **CC2** did not reach the catalytic W82 in the AChE catalytic anionic site (CAS) and can interact with F295 and W286 (Figure S1). On the other hand, only compound **CC2** can make $\pi-\pi$ interactions with the catalytic W82 residue towards BChE (Figure S2), in agreement with the experimental data.

3. CONCLUSIONS

In summary, a series of 10 coumarin−chalcones substituted with halogens were synthesized and tested for MAOs, ChEs, and BACE-1 inhibitory activities. All of the compounds showed better MAO-B inhibitory activity compared to MAO-A. **CC1** and **CC2** in particular showed the best MAO-B inhibition. The nature and orientation of the halogen group at the phenyl **B** ring were responsible for the MAO-B and ChE inhibitory activities. From the series, the halogen atom substituted at the *ortho* position potentially inhibited MAO-B with IC_{50} values of 0.51, 7.76, and 23.6 μM for 2-Cl, 2-F = 7.76, and 2-Br, respectively, and **CC2** moderately inhibited MAO-B. In addition, compound **CC1** with an unsubstituted phenyl ring showed better MAO-B inhibition with an IC_{50} value of 0.51 μM. None of the compounds effectively inhibited MAO-A, AChE, and BChE, except for **CC2** and **CC3** inhibiting BChE with IC_{50} values of 7.00 (SI > 5.73 over AChE) and 11.8 μM, respectively. It is concluded that **CC1** and **CC2** are selective and competitive inhibitors of MAO-B, and **CC2** is a selective and competitive inhibitor of BChE. Moreover, the biological safety of both **CC1** and **CC2** depicts the nontoxic behavior of the compounds at the EC50 level. We believe that this study provides the first evidence for the synthesized chalcone derivatives, **CC1** and **CC2**, which have a free radical scavenging effect, thereby inhibiting oxidative stress in a disease condition. Therefore, this study may provide information for the design and development of a novel potent drug against neurodegenerative diseases.

4. MATERIALS AND METHODS

4.1. Synthesis. The chemicals for the synthesis were purchased from Sigma-Aldrich (St. Louis, MO). Acetylcoumarin (0.01 mol) and substituted benzaldehyde (0.01 mol) were dissolved in 50 mL of ethanol in the presence of piperidine (0.001 mol) as a catalyst, and the mixture was stirred for 10 min at room temperature. It was refluxed for 8−10 h with a constant temperature at 80 °C and cooled, and the solution was then filtered, washed with water, and dried. The product was recrystallized with ethanol to obtain pure crystals.[62,63] The purities of the compounds were analyzed by thin-layer chromatography [10:90 ethylacetate/hexane] (Scheme 1).

4.2. Enzyme Assays. MAO activities were assayed using recombinant human MAO-A and MAO-B in the presence of kynuramine (0.06 mM) and benzylamine (0.3 mM) as substrates, respectively, as described previously.[64] The substrate concentrations were 1.5× and 2.3× K_m, respectively; the K_m values of these substrates were 0.041 and 0.13 mM, respectively. AChE and BChE activities were measured using the enzymes from Electrophorus electricus Type VI-S and equine serum, respectively, in the presence of 0.5 mM acetylthiocholine iodide (ATCI) and butyrylthiocholine iodide (BTCI) as substrates, respectively, and 0.5 mM 5,5′-dithiobis-(2-nitrobenzoic acid) (DTNB) as a color-developing agent, as described previously.[65,66] Inhibitory activities were measured

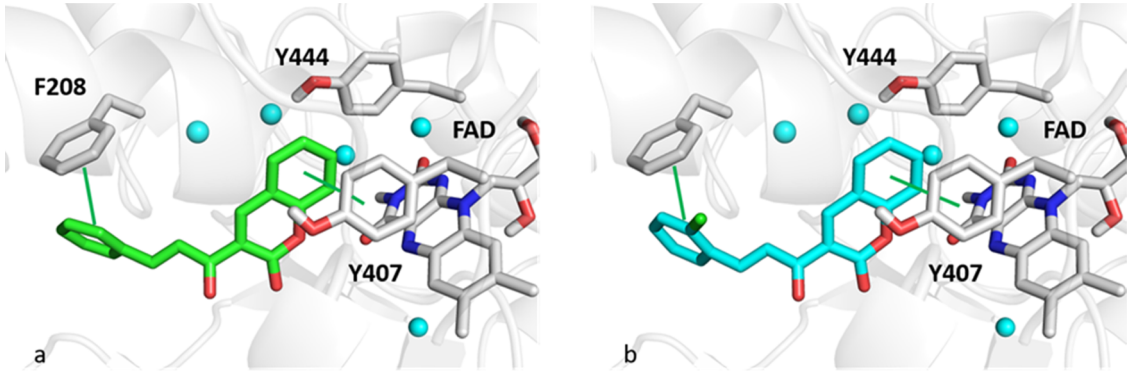

Figure 9. Zoomed-in view of an MAO-A binding pocket. Panels (a) and (b) show the best pose returned from the docking analysis of **CC1** (green sticks) and **CC2** (cyan sticks), respectively. Cyan spheres indicate water molecules. Green lines show $\pi-\pi$ contacts.

https://doi.org/10.1021/acsomega.1c04252
ACS Omega 2021, 6, 28182−28193

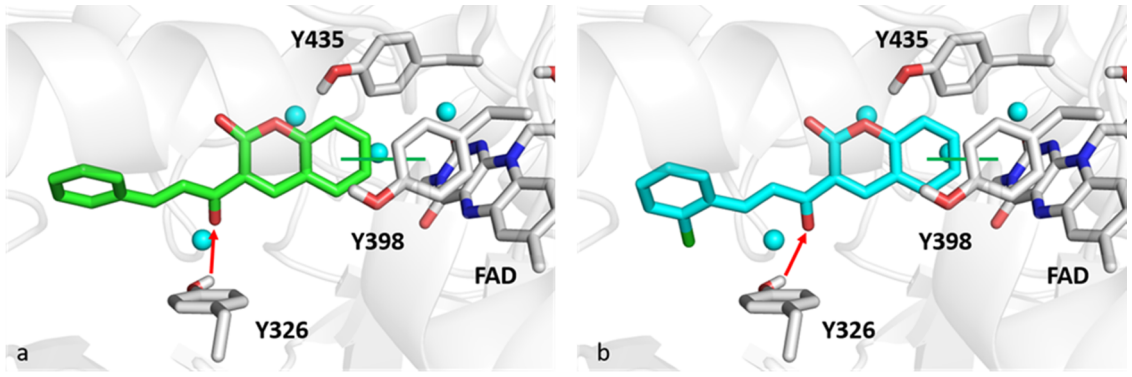

Figure 10. Zoomed-in view of an MAO-B binding pocket. Panels (a) and (b) show the best pose returned from docking analysis of **CC1** (green sticks) and **CC2** (cyan sticks), respectively. Cyan spheres indicate water molecules. Green lines and red arrows show $\pi-\pi$ contacts and hydrogen bonds, respectively.

Scheme 1. Synthetic Route for CC Series

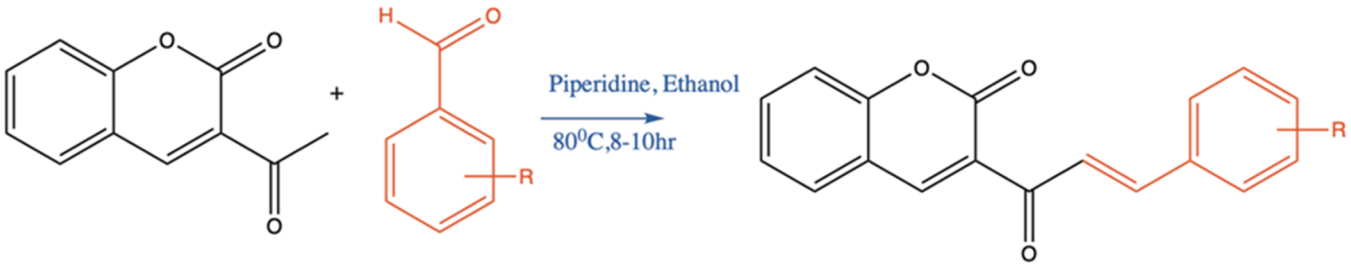

CC1-CC10

	R		R
CC1	H	CC6	3-Br
CC2	2-Cl	CC7	4-Br
CC3	3-Cl	CC8	2-F
CC4	4-Cl	CC9	3-F
CC5	2-Br	CC10	4-F

after preincubating the substrates and inhibitors for 15 min. BACE-1 activity was measured using a BACE-1 activity detection kit at excitation 320 nm and emission 405 nm using a fluorescence spectrometer (FS-2, Scinco, Seoul, Korea), as described previously.[67] The enzymes and chemicals were purchased from Sigma-Aldrich (St. Louis, MO).

4.3. Analysis of Enzyme Inhibitions and Kinetics. The inhibitory activities of 10 compounds against MAO-A, MAO-B, AChE, BChE, and BACE-1 were first observed at a concentration of 10 μM, and then IC_{50} values were determined for the compounds, of which the residual activities were <50%. Reversibility and kinetic studies were performed on the most potent inhibitors, i.e., **CC1** and **CC2** for MAO-B and **CC2** for BChE, as previously described.[68] Kinetic experiments were conducted at five concentrations of substrates and three inhibitor concentrations.

4.4. Analysis of Inhibitor Reversibility. The reversibility of compounds **CC1** and **CC2** was analyzed using a dialysis method after preincubating with MAO-B for 30 min, as previously described.[69] In the reversibility of MAO-B, the concentrations used were 1.00 and 1.40 μM for **CC1** and **CC2**, respectively, 0.20 μM for lazabemide (a reversible MAO-B reference inhibitor), and 0.28 μM for pargyline (an irreversible MAO-B reference inhibitor). In BChE experiments, the concentration used was 14.0 μM for **CC2** and 0.36 μM for donepezil (a reversible BChE reference inhibitor).[70] The relative activities for the undialyzed (AU) and dialyzed (AD) samples were compared to determine the reversibility patterns.[71]

4.5. Cytotoxicity and ROS Assay. The lead molecules **CC1** and **CC2** were evaluated for cytotoxicity and ROS scavenging potentiality, as previously described[72,73] and as described shortly in the Supporting Information.

4.6. Computational Studies. The X-ray crystal structures of MAO-A and MAO-B were taken from the Protein Data Bank with entries 2Z5X and 2V5Z, respectively.[74,75] These structures were treated with the Protein Preparation Wizard available in the Schrödinger Suite to predict the correct protonation states, remove nonfunctional water molecules, and minimize the total energy.[76,77] Ligands were treated with the Ligprep Tool to generate all possible tautomers and the allowed conformations. The grid boxes were centered on the center of mass of the cognate ligands, and the SP docking protocol was set when using the GLIDE software. Finally, an

https://doi.org/10.1021/acsomega.1c04252
ACS Omega 2021, 6, 28182−28193

estimation of the free energy of binding was done by employing the Molecular Mechanics Generalized Born Surface Area (MM-GBSA) approach.[78,79]

■ ASSOCIATED CONTENT

Supporting Information

The Supporting Information is available free of charge at https://pubs.acs.org/doi/10.1021/acsomega.1c04252.

Spectral data of ^{1}H- and ^{13}C-NMR and MS chromatograms for compounds (Figures S1−S21); zoomed-in views (Figures S22 and S23); and docking score and MMSBSA values (Tables S1 and S2) (PDF)

■ AUTHOR INFORMATION

Corresponding Authors

Hoon Kim − *Department of Pharmacy, and Research Institute of Life Pharmaceutical Sciences, Sunchon National University, Suncheon 57922, Republic of Korea;* orcid.org/0000-0002-7203-3712; Email: hoon@sunchon.ac.kr

Bijo Mathew − *Department of Pharmaceutical Chemistry, Amrita School of Pharmacy, Amrita Vishwa Vidyapeetham, AIMS Health Sciences Campus, Kochi 682 041, India;* Email: bijomathew@aims.amrita.edu, bijovilaventgu@gmail.com

Authors

Nisha Abdul Rehuman − *Department of Pharmaceutical Chemistry, Dr. Joseph Mar Thoma Institute of Pharmaceutical Sciences & Research, Alappuzha, Kerala 690503, India*

Jong Min Oh − *Department of Pharmacy, and Research Institute of Life Pharmaceutical Sciences, Sunchon National University, Suncheon 57922, Republic of Korea*

Lekshmi R. Nath − *Department of Pharmacognosy, Amrita School of Pharmacy, Amrita Vishwa Vidyapeetham, Kochi 682, India*

Ahmed Khames − *Department of Pharmaceutics and Industrial Pharmacy, College of Pharmacy, Taif University, Taif 21944, Saudi Arabia*

Mohamed A. Abdelgawad − *Department of Pharmaceutical Chemistry, College of Pharmacy, Jouf University, Sakaka, Al Jouf 72341, Saudi Arabia*

Nicola Gambacorta − *Dipartimento di Farmacia—Scienze del Farmaco, Università degli Studi di Bari "Aldo Moro", I-70125 Bari, Italy*

Orazio Nicolotti − *Dipartimento di Farmacia—Scienze del Farmaco, Università degli Studi di Bari "Aldo Moro", I-70125 Bari, Italy;* orcid.org/0000-0001-6533-5539

Rakesh Kumar Jat − *Department of Pharmaceutical Chemistry, JJTU University, Jhunjhunu 333001, India*

Complete contact information is available at: https://pubs.acs.org/10.1021/acsomega.1c04252

Author Contributions

◆N.A.R., J.M.O., and B.M. contributed equally to this work.

Notes

The authors declare no competing financial interest.

■ ACKNOWLEDGMENTS

This study was supported by the National Research Foundation of Korea (NRF) grant provided by the Korean Government (NRF-2019R1A2C1088967 to H.K.), Republic of Korea, and by a grant from Amrita Vishwa Vidyapeetham University (Seed Grant Number K-PHAR-20-628 to B.M.). The authors acknowledge Taif University Researchers Supporting Project number (TURSP-2020/68), Taif University, Taif, Saudi Arabia.

■ REFERENCES

(1) Hampel, H.; Prvulovic, D.; Teipel, S.; Jessen, F.; Luckhaus, C.; Frolich, L.; Riepe, M. W.; Dodel, R.; Leyhe, T.; Bertram, L.; Hoffmann, W.; Faltraco, F. The future of Alzheimer's disease: the next 10 years. *Prog. Neurobiol.* **2011**, *95*, 718−728.

(2) Massoud, F.; Gauthier, S. Update on the pharmacological treatment of Alzheimer's disease. *Curr. Neuropharmacol.* **2010**, *8*, 69−80.

(3) Mathew, B.; Kim, H. Inhibitors of monoamine oxidase and acetylcholinesterase as a front runner in CNS drug discovery. *Comb. Chem. High Throughput Screening* **2020**, *23*, 834−835.

(4) Sharma, P.; Singh, B.; Mathew, B. An update of synthetic approaches and structure-activity relationships of various classes of human MAO-B inhibitors. *ChemistrySelect* **2021**, *6*, 1404−1429.

(5) Inestrosa, N. C.; Alvarez, A.; Perez, C. A.; Moreno, R. D.; Vicente, M.; Linker, C.; Casanueva, O. I.; Soto, C.; Garrido, J. Acetylcholinesterase accelerates assembly of amyloid-beta- peptides into Alzheimer's fibrils: possible role of the peripheral site of the enzyme. *Neuron* **1996**, *16*, 881−891.

(6) Alvarez, A.; Alarcon, R.; Opazo, C.; Campos, E. O.; Munoz, F. J.; Calderon, F. H.; Dajas, F.; Gentry, M. K.; Doctor, B. P.; De Mello, F. G.; Inestrosa, N. C. Stable complexes involving acetylcholinesterase and amyloid-beta peptide change the biochemical properties of the enzyme and increase the neurotoxicity of Alzheimer's fibrils. *J. Neurosci.* **1998**, *18*, 3213−3223.

(7) Nordberg, A.; Alafuzoff, I.; Winblad, B. Nicotinic and muscarinic subtypes in the human brain: changes with aging anddementia. *J. Neurosci. Res.* **1992**, *31*, 103−111.

(8) Zheng, W. H.; Bastianetto, S.; Mennicken, F.; Ma, W.; Kar, S. Amyloid beta peptide induces tau phosphorylation and loss of cholinergic neurons in rat primary septal cultures. *Neuroscience* **2002**, *115*, 201−211.

(9) Kar, S.; Slowikowski, S. P.; Westaway, D.; Mount, H. T. Interactions between beta-amyloid and central cholinergic neurons: implications for Alzheimer's disease. *J. Psychiatry Neurosci.* **2004**, *29*, 427−441.

(10) Cavalli, A.; Bolognesi, M. L.; Minarini, A.; Rosini, M.; Tumiatti, V.; Recanatini, M.; Melchiorre, C. Multi-target-directed ligands to combat neurodegenerative diseases. *J. Med. Chem.* **2008**, *51*, 347−372.

(11) Bajda, M.; Guzior, N.; Ignasik, M.; Malawska, B. Multi- target-directed ligands in Alzheimer's disease treatment. *Curr. Med. Chem.* **2011**, *18*, 4949−4975.

(12) Leon, R.; Marco-Contelles, J. A step further towards multitarget drugs for Alzheimer and neuronal vascular diseases: targeting the cholinergic system, amyloid-beta aggregation and Ca$^{(2+)}$ dyshomeostasis. *Curr. Med. Chem.* **2011**, *18*, 552−576.

(13) De Strooper, B. Proteases and proteolysis in Alzheimer disease: a multifactorial view on the disease process. *Physiol. Rev.* **2010**, *90*, 465−494.

(14) Francis, P. T.; Palmer, A. M.; Snape, M.; Wilcock, G. K. The cholinergic hypothesis of Alzheimer's disease: a review of progress. *J. Neurol., Neurosurg. Psychiatry* **1999**, *66*, 137−147.

(15) Lipton, S. A. Pathologically-activated therapeutics for neuroprotection: mechanism of NMDA receptor block by memantine and S-nitrosylation. *Curr. Drug Targets* **2007**, *8*, 621−632.

(16) Csermely, P.; Agoston, V.; Pongor, S. The efficiency of multi-target drugs: the network approach might help drug design. *Trends Pharmacol. Sci.* **2005**, *26*, 178−182.

(17) Geldenhuys, W. J.; Van der Schyf, C. J. Designing drugs with multi- target activity: the next step in the treatment of neuro-

degenerative disorders. *Expert Opin. Drug Discovery* **2013**, *8*, 115−129.
(18) Zhuang, C.; Zhang, W.; Sheng, C.; Zhang, W.; Xing, C.; Miao, Z. Chalcone: A Privileged Structure in Medicinal Chemistry. *Chem. Rev.* **2017**, *117*, 7762−7810.
(19) Guglielmi, P.; Mathew, B.; Secci, D.; Carradori, S. Chalcones: Unearthing their therapeutic possibility as monoamine oxidase B inhibitors. *Eur. J. Med. Chem.* **2020**, *205*, No. 112650.
(20) Irfan, R.; Mousavi, S.; Alazmi, M.; Saleem, R. S. Z. A Comprehensive review of aminochalcones. *Molecules* **2020**, *25*, No. 5381.
(21) Borges, F.; Roleira, F.; Milhazes, N.; Santana, L.; Uriarte, E. Simple coumarins and analogues in medicinal chemistry: occurrence, synthesis and biological activity. *Curr. Med. Chem.* **2005**, *12*, 887−916.
(22) Kostova, I.; Bhatia, S.; Grigorov, P.; Balkansky, S.; Parmar, V. S.; Prasad, A. K.; Saso, L. Coumarins as antioxidants. *Curr. Med. Chem.* **2011**, *18*, 3929−3951.
(23) Fylaktakidou, K. C.; Hadjipavlou-Litina, D. J.; Litinas, K. E.; Nico- laides, D. N. Natural and synthetic coumarin derivatives with anti-inflammatory/antioxidant activities. *Curr. Pharm. Des.* **2004**, *10*, 3813−3833.
(24) Atmaca, M.; Bilgin, H. M.; Obay, B. D.; Diken, H.; Kelle, M.; Kale, E. The hepatoprotective effect of coumarin and coumarin derivates on carbon tetrachloride-induced hepatic injury by antioxidative activities in rats. *J. Physiol. Biochem.* **2011**, *67*, 569−576.
(25) Liaras, K.; Geronikaki, A.; Glamoclija, J.; Ciric, A.; Sokovic, M. Thiazole-based chalcones as potent antimicrobial agents. Synthesis and biological evaluation. *Bioorg. Med. Chem.* **2011**, *19*, 3135−3140.
(26) Liu, Z. J.; Wang, Y.; Lin, H. F.; Zuo, D. Z.; Wang, L. H.; Zhao, Y. F.; Gong, P. Design, synthesis and biological evaluation of novel thieno[3,2-d] pyrimidine derivatives containing diaryl urea moiety as potent antitumor agents. *Eur. J. Med. Chem.* **2014**, *85*, 215−227.
(27) Emami, S.; Dadashpour, S. Current developments of coumarin-based anti-cancer agents in medicinal chemistry. *Eur. J. Med. Chem.* **2015**, *102*, 611−630.
(28) Chimenti, F.; Secci, D.; Bolasco, A.; Chimenti, P.; Bizzarri, B.; Granese, A.; Carradori, S.; Yáñez, M.; Orallo, F.; Ortuso, F.; Alcaro, S. Synthesis, molecular modeling, and selective inhibitory activity against human monoamine oxidases of 3-carboxamido-7-substituted coumarins. *J. Med. Chem.* **2009**, *52*, 1935−1942.
(29) Kurt, B. Z.; Gazioglu, I.; Dag, A.; Salmas, R. E.; Kayik, G.; Durdagi, S.; Sonmez, F. Synthesis, anticholinesterase activity and molecular modeling study of novel carbamate-substituted thy- mol/carvacrol derivatives. *Bioorg. Med. Chem.* **2017**, *25*, 1352−1363.
(30) Hammuda, A.; Shalaby, R.; Rovida, S.; Edmondson, D. E.; Binda, C.; Khalil, A. Design and synthesis of novel chalcones as potent selective monoamine oxidase-B inhibitors. *Eur. J. Med. Chem.* **2016**, *114*, 162−169.
(31) Hitge, R.; Smit, S.; Petzer, A.; Petzer, J. P. Evaluation of nitrocatechol chalcone and pyrazoline derivatives as inhibitors of catechol-O-methyltransferase and monoamine oxidase. *Bioorg. Med. Chem. Lett.* **2020**, *30*, No. 127188.
(32) Kong, Z.; Sun, D.; Jiang, Y.; Hu, Y. Design, synthesis, and evaluation of 1, 4-benzodioxan-substituted chalcones as selective and reversible inhibitors of human monoamine oxidase B. *J. Enzyme Inhib. Med. Chem.* **2020**, *35*, 1513−1523.
(33) Chimenti, F.; Fioravanti, R.; Bolasco, A.; Chimenti, P.; Secci, D.; Rossi, F.; Yáñez, M.; Orallo, F.; Ortuso, F.; Alcaro, S. Chalcones: a valid scaffold for monoamine oxidases inhibitors. *J. Med. Chem.* **2009**, *52*, 2818−2824.
(34) Minders, C.; Petzer, J. P.; Petzer, A.; Lourens, A. C. Monoamine oxidase inhibitory activities of heterocyclic chalcones. *Bioorg. Med. Chem. Lett.* **2015**, *25*, 5270−5276.
(35) Sasidharan, R.; Manju, S. L.; Uçar, G.; Baysal, I.; Mathew, B. Identification of indole-based chalcones: discovery of a potent, selective, and reversible class of MAO-B inhibitors. *Arch. Pharm.* **2016**, *349*, 627−637.
(36) Mathew, B.; Haridas, A.; Uçar, G.; Baysal, I.; Joy, M.; Mathew, G. E.; Lakshmanan, B.; Jayaprakash, V. Synthesis, biochemistry, and computational studies of brominated thienyl chalcones: A new class of reversible MAO-B Inhibitors. *Chem. Med. Chem.* **2016**, *11*, 1161−1171.
(37) Xiao, G.; Li, Y.; Qiang, X.; Xu, R.; Zheng, Y.; Cao, Z.; Luo, L.; Yang, X.; Sang, Z.; Su, F.; Deng, Y. Design, synthesis and biological evaluation of 4′-aminochalcone-rivastigmine hybrids as multifunctional agents for the treatment of Alzheimer's disease. *Bioorg. Med. Chem.* **2017**, *25*, 1030−1041.
(38) Cao, Z.; Yang, J.; Xu, R.; Song, Q.; Zhang, X.; Liu, H.; Qiang, X.; Li, Y.; Tan, Z.; Deng, Y. Design, synthesis and evaluation of 4′-OH-flurbiprofen-chalcone hybrids as potential multifunctional agents for Alzheimer's disease treatment. *Bioorg. Med. Chem.* **2018**, *26*, 1102−1115.
(39) Robinson, S. J.; Petzer, J. P.; Petzer, A.; Bergh, J. J.; Lourens, A. C. Selected furanochalcones as inhibitors of monoamine oxidase. *Bioorg. Med. Chem. Lett.* **2013**, *23*, 4985−4989.
(40) Jo, G.; Ahn, S.; Kim, B. G.; Park, H. R.; Kim, Y. H.; Choo, H. A.; Koh, D.; Chong, Y.; Ahn, J. H.; Lim, Y. Chromenylchalcones with inhibitory effects on monoamine oxidase B. *Bioorg. Med. Chem.* **2013**, *21*, 7890−7897.
(41) Mellado, M.; González, C.; Mella, J.; Aguilar, L. F.; Viña, D.; Uriarte, E.; Cuellar, M.; Matos, M. J. Combined 3D-QSAR and docking analysis for the design and synthesis of chalcones as potent and selective monoamine oxidase B inhibitors. *Bioorg. Chem.* **2021**, *108*, No. 104689.
(42) Mathew, B.; Baek, S. C.; Thomas Parambi, D. G.; Lee, J. P.; Mathew, G. E.; Jayanthi, S.; Vinod, D.; Rapheal, C.; Devikrishna, V.; Kondarath, S. S.; Uddin, M. S.; Kim, H. Potent and highly selective dual-targeting monoamine oxidase-B inhibitors: Fluorinated chalcones of morpholine versus imidazole. *Arch. Pharm.* **2019**, *352*, No. 1800309.
(43) Parambi, D. G. T.; Oh, J. M.; Baek, S. C.; Lee, J. P.; Tondo, A. R.; Nicolotti, O.; Kim, H.; Mathew, B. Design, synthesis and biological evaluation of oxygenated chalcones as potent and selective MAO-B inhibitors. *Bioorg. Chem.* **2019**, *93*, No. 103335.
(44) Sang, Z.; Wang, K.; Zhang, P.; Shi, J.; Liu, W.; Tan, Z. Design, synthesis, in-silico and biological evaluation of novel chalcone derivatives as multi-function agents for the treatment of Alzheimer's disease. *Eur. J. Med. Chem.* **2019**, *180*, 238−252.
(45) Zhang, X.; Song, Q.; Cao, Z.; Li, Y.; Tian, C.; Yang, Z.; Zhang, H.; Deng, Y. Design, synthesis and evaluation of chalcone Mannich base derivatives as multifunctional agents for the potential treatment of Alzheimer's disease. *Bioorg. Chem.* **2019**, *87*, 395−408.
(46) Shalaby, R.; Petzer, J. P.; Petzer, A.; Ashraf, U. M.; Atari, E.; Alasmari, F.; Kumarasamy, S.; Sari, Y.; Khalil, A. SAR and molecular mechanism studies of monoamine oxidase inhibition by selected chalcone analogs. *J. Enzyme Inhib. Med. Chem.* **2019**, *34*, 863−876.
(47) Bai, P.; Wang, K.; Zhang, P.; Shi, J.; Cheng, X.; Zhang, Q.; Zheng, C.; Cheng, Y.; Yang, J.; Lu, X.; Sang, Z. Development of chalcone-O-alkylamine derivatives as multifunctional agents against Alzheimer's disease. *Eur. J. Med. Chem.* **2019**, *183*, No. 111737.
(48) Mathew, B. Privileged pharmacophore of FDA approved drugs in combination with chalcone framework: A new hope for Alzheimer's treatment. *Comb. Chem. High Throughput Screening* **2020**, *23*, 842−846.
(49) Nair, A. S.; Oh, J. M.; Koyiparambath, V. P.; Kumar, S.; Sudevan, S. T.; Soremekun, O.; Soliman, M. E.; Khames, A.; Abdelgawad, M. A.; Pappachen, L. K.; Mathew, B.; Kim, H. Development of halogenated pyrazolines as selective monoamine oxidase-B Inhibitors: Deciphering via molecular dynamics approach. *Molecules* **2021**, *26*, No. 3264.
(50) Mathew, B.; Carradori, S.; Guglielmi, P.; Uddin, M. S.; Kim, H. New aspects of monoamine oxidase b inhibitors: The key role of halogens to open the golden door. *Curr. Med. Chem.* **2020**, *28*, 266−283.

https://doi.org/10.1021/acsomega.1c04252
ACS Omega 2021, 6, 28182−28193

(51) Wei, H.; Ruan, J. L.; Zhang, X. J. Coumarin-chalcone hybrids: promising agents with diverse pharmacological properties. *RSC Adv.* **2016**, *6*, 10846−10860.
(52) Serdiuk, I. E.; Wera, M.; Roshal, A. D. Structural and spectral features of 4′-substituted 2′-hydroxychalcones in solutions and crystals: Spectroscopic and theoretical investigations. *J. Phys. Chem. A* **2018**, *122*, 2030−2038.
(53) Sahu, N. K.; Balbhadra, S. S.; Choudhary, J.; Kohli, D. V. Exploring pharmacological significance of chalcone scaffold: a review. *Curr. Med. Chem.* **2012**, *19*, 209−225.
(54) Moya-Alvarado, G.; Yañez, O.; Morales, N.; González-González, A.; Areche, C.; Núñez, M. T.; Fierro, A.; García-Beltrán, O. Coumarin-chalcone hybrids as inhibitors of MAO-B: Biological activity and in silico studies. *Molecules* **2021**, *26*, No. 2430.
(55) Khode, S.; Maddi, V.; Aragade, P.; Palkar, M.; Ronad, P. K.; Mamledesai, S.; Thippeswamy, A. H.; Satyanarayana, D. Synthesis and pharmacological evaluation of a novel series of 5-(substituted)aryl-3-(3-coumarinyl)-1-phenyl-2-pyrazolines as novel anti-inflammatory and analgesic agents. *Eur. J. Med. Chem.* **2009**, *44*, 1682−1688.
(56) Ajani, O. O.; Nwinyi, O. C. Microwave-assisted synthesis and evaluation of antimicrobial activity of 3-{3-(s-aryl and s-hetero-aromatic) acryloyl}-2H-chromen-2-one derivatives. *J. Heterocycl. Chem.* **2010**, *47*, 179−187.
(57) Mathew, B.; Adeniyi, A. A.; Joy, M.; Mathew, G. E.; Ashona Singh-Pillay, A. S.; Sudarsanakumar, C.; Soliman, M. E. S.; Suresh, J. Anti-oxidant behavior of functionalized chalcone-a combined quantum chemical and crystallographic structural investigation. *J. Mol. Struct.* **2017**, *1146*, 301−308.
(58) Carradori, S.; Secci, D.; Petzer, J. P. MAO inhibitors and their wider applications: a patent review. *Expert Opin. Ther. Pat.* **2018**, *28*, 211−226.
(59) Tripathi, A. C.; Upadhyay, S.; Paliwal, S.; Saraf, S. K. Privileged scaffolds as MAO inhibitors: Retrospect and prospects. *Eur. J. Med. Chem.* **2018**, *145*, 445−497.
(60) Kim, S.; Kim, M.; Kang, M. C.; Lee, H. H. L.; Cho, C. H.; Choi, I.; Park, Y.; Lee, S. H. Antioxidant effects of turmeric leaf extract against hydrogen peroxide-induced oxidative stress in vitro in vero cells and in vivo in zebrafish. *Antioxidants* **2021**, *10*, No. 112.
(61) Cenini, G.; Lloret, A.; Cascella, R. Oxidative stress in neurodegenerative diseases: From a mitochondrial point of view. *Oxid. Med. Cell. Longevity* **2019**, No. 2105607.
(62) Kumar, G.; Siva Krishna, V.; Sriram, D.; Jachak, S. M. Pyrazole-coumarin and pyrazole-quinoline chalcones as potential antitubercular agents. *Arch. Pharm.* **2020**, *353*, No. 2000077.
(63) Rodriguez, S. V.; Guíñez, R. F.; Matos, M. J.; Azar, C. O.; Maya, J. D.; Santana, L.; Borges, F. Synthesis and trypanocidal properties of new coumarin-chalcone derivatives. *Med. Chem.* **2015**, *5*, 173−177.
(64) Oh, J. M.; Özdemir, Z.; Büyüktuncel, S. E.; Uysal, M.; Mohamed, A. A.; Musa, A.; Gambacorta, N.; Nicolotti, O.; Mathew, B.; Kim, H.; et al. Design, synthesis, and biological evaluation of pyridazinones containing the (2-fluorophenyl) piperazine moiety as selective MAO-B inhibitors. *Molecules* **2020**, *25*, No. 5371.
(65) Baek, S. C.; Park, M. H.; Ryu, H. W.; Lee, J. P.; Kang, M. G.; Park, D.; Park, C. M.; Oh, S. R.; Kim, H. Rhamnocitrin isolated from *Prunus padus* var. seoulensis: A potent and selective reversible inhibitor of human monoamine oxidase A. *Bioorg. Chem.* **2019**, *83*, 317−325.
(66) Lee, J. P.; Kang, M. G.; Lee, J. Y.; Oh, J. M.; Baek, S. C.; Leem, H. H.; Park, D.; Cho, M. L.; Kim, H. Potent inhibition of acetylcholinesterase by sargachromanol I from *Sargassum siliquastrum* and by selected natural compounds. *Bioorg. Chem.* **2019**, *89*, No. 103043.
(67) Jeong, G. S.; Kang, M. G.; Han, S. A.; Noh, J. I.; Park, J. E.; Nam, S. J.; Park, D.; Yee, S. T.; Kim, H. Selective inhibition of human monoamine oxidase B by 5-hydroxy-2-methyl-chroman-4-one isolated from an endogenous lichen fungus *Daldinia fissa*. *J. Fungi* **2021**, *7*, No. 84.
(68) Lee, H. W.; Ryu, H. W.; Kang, M. G.; Park, D.; Oh, S. R.; Kim, H. Potent selective monoamine oxidase B inhibition by maackiain, a pterocarpan from the roots of *Sophora flavescens*. *Bioorg. Med. Chem. Lett.* **2016**, *26*, 4714−4719.
(69) Vishal, P. K.; Oh, J. M.; Khames, A.; Abdelgawad, M. A.; Nair, A. S.; Nath, L. R.; Gambacorta, N.; Ciriaco, F.; Nicolotti, O.; Kim, H.; Mathew, B. Trimethoxylated halogenated chalcones as dual inhibitors of MAO-B and BACE-1 for the treatment of neurodegenerative disorders. *Pharmaceutics* **2021**, *13*, No. 850.
(70) Mathew, B.; Oh, J. M.; Baty, R. S.; Batiha, G. E.; Parambi, D.G.T.; Gambacorta, N.; Nicolotti, O.; Kim, H. Piperazine-substituted chalcones: a new class of MAO-B, AChE, and BACE-1 inhibitors for the treatment of neurological disorders. *Environ. Sci. Pollut. Res.* **2021**, *28*, 38855−38866.
(71) Sellitepe, H. E.; Oh, J. M.; Doğan, İ.S.; Yildirim, S.; Aksel, A. B.; Jeong, G. S.; Khames, A.; Abdelgawad, M. A.; Gambacorta, N.; Nicolotti, O.; Mathew, B.; Kim, H. Synthesis of *N*′-(4-/3-/2-/Non-substituted benzylidene)-4-[(4-methylphenyl)sulfonyloxy] benzohydrazides and evaluation of their inhibitory activities against monoamine oxidases and *β*-secretase. *Appl. Sci.* **2021**, *11*, No. 5830.
(72) Fotakis, G.; Timbrell, J. A. In vitro cytotoxicity assays: comparison of LDH, neutral red, MTT and protein assay in hepatoma cell lines following exposure to cadmium chloride. *Toxicol. Lett.* **2006**, *160*, 171−177.
(73) Jambunathan, N. Determination and detection of reactive oxygen species (ROS), lipid peroxidation, and electrolyte leakage in plants. *Methods Mol. Biol.* **2010**, *639*, 292−298.
(74) Son, S. Y.; Ma, J.; Kondou, Y.; Yoshimura, M.; Yamashita, E.; Tsukihara, T. Structure of human monoamine oxidase A at 2.2-A resolution: The control of opening the entry for substrates/inhibitors. *Proc. Natl. Acad. Sci. U.S.A.* **2008**, *105*, 5739−5744.
(75) Binda, C.; Wang, J.; Pisani, L.; Caccia, C.; Carotti, A.; Salvati, P.; Edmondson, D. E.; Mattevi, A. Structures of human monoamine oxidase B complexes with selective noncovalent inhibitors: safinamide and coumarin analogs. *J. Med. Chem.* **2007**, *50*, 5848−5852.
(76) Friesner, R. A.; Banks, J. L.; Murphy, R. B.; Halgren, T. A.; Klicic, J. J.; Mainz, D. T.; Repasky, M. P.; Knoll, E. H.; Shelley, M.; Perry, J. K.; Shaw, D. E.; Francis, P.; Shenkin, P. S. Glide: A new approach for rapid, accurate docking and scoring. 1. Method and assessment of docking accuracy. *J. Med. Chem.* **2004**, *47*, 1739−1749.
(77) Schrödinger Release 2020-4: Protein Preparation Wizard; Epik, Schrödinger, LLC, New York, NY, 2016; Impact, Schrödinger, LLC, New York, NY, 2016; Prime, Schrödinger, LLC: New York, NY, 2020.
(78) Madhavi Sastry, G.; Adzhigirey, M.; Day, T.; Annabhimoju, R.; Sherman, W. Protein and Ligand Preparation: Parameters, protocols, and influence on virtual screening enrichments. *J. Comput.-Aided Mol. Des.* **2013**, *27*, 221−234.
(79) *Schrödinger Release 2020-4: LigPrep*; Schrödinger, LLC: New York, NY, 2020.

https://doi.org/10.1021/acsomega.1c04252
ACS Omega 2021, 6, 28182−28193